

# Transport Properties and Mechanisms Modulated by Doping Ratio of Ce in $\text{La}_{1-x}\text{Ce}_x\text{MnO}_3$ Electronic-doped Films

Niu Liwei, Chen Changle, Wang Jianyuan, Jin Kexin

Shaanxi Key Laboratory for Condensed Matter Structure and Properties, Northwestern Polytechnical University, Xi'an 710129, China

**Abstract:** We performed the experimental studies on  $\text{La}_{1-x}\text{Ce}_x\text{MnO}_3$  to investigate transport properties and field-induced transport mechanisms in electronic doped perovskite films.  $\text{La}_{1-x}\text{Ce}_x\text{MnO}_3$  films exhibit significant metal-insulator transition, which can be modulated by the doping ratio of Ce. Resistance-temperature curves indicate that the magnetic domains and electron-electron scattering mainly contribute to the transport mechanism in the low temperature region, while the hopping conduction of small polaron becomes the dominating factor at the high temperatures. Laser irradiation is found to induce the shift of metal-insulator transition temperature towards the lower temperature region due to the coexistence of ferromagnetic (FM) metallic phase and paramagnetic (PM) insulating phase in  $\text{La}_{1-x}\text{Ce}_x\text{MnO}_3$  films. The higher laser intensity gives rise to more significant change in resistance. Furthermore, magnetoresistance effect can be affected by different doping ratios of Ce in  $\text{La}_{1-x}\text{Ce}_x\text{MnO}_3$  films because of the MIT transition.

**Key words:** perovskite manganites; transport mechanism; metal-insulator transition; colossal magnetoresistance effect

Microelectronics information technology has greatly promoted the applications and innovations of semiconductor materials and devices. To meet requirements of technical applications, the semiconductor microelectronics devices are getting smaller with more and more highly integrated and diversified functions. However, the physical properties of traditional semiconductor materials can only make relatively single-functional devices, which imposes the restrictions on their device applications<sup>[1]</sup>. Therefore, the development of new multi-functional semiconductor materials has become the challenge for the new electronic information industry. Among those multi-functional semiconductor materials, perovskite oxides, especially the transition metal oxides, have been attracting investigation due to their strongly correlated electron systems recently<sup>[2-6]</sup>. Due to the inherent coupling dynamics, the charge, spin, orbit and lattice can induce the complex structures and electronic phases, which exhibit many novel physical phenomena in the oxide materials, such as the colossal magnetoresistance (CMR) effect<sup>[7,8]</sup>, the ordered domain and microstructure, the field induced metal-insulator

transition (MIT)<sup>[9]</sup>, and the electronic phase separation (EPS)<sup>[10,11]</sup>, enabling these transition metal oxides favorable multi-functional semiconductors. According to many experiments and analysis on the interactions of the manganese oxides systems (double exchange interaction, super exchange interaction, electron-phonon coupling, spin-phonon coupling), it has been found that the competitions between different interactions produce the complex structure transition and electromagnetic phase diagram, and induce the new novel phenomena in manganese oxides systems, which present prospect in the application of multi-functional semiconductor devices.

Von Helmolt et al<sup>[12]</sup> proposed the existence of magnetoresistance (MR) effect in  $\text{La}_{1-x}\text{Ba}_x\text{MnO}_3$  films. Jin et al<sup>[13]</sup> prepared  $\text{La}_{0.16}\text{Ba}_{0.33}\text{MnO}_3$  thin films by pulsed laser deposition (PLD) technology, and they observed the magnetoresistance effect of 127000% at the temperature of 77 K under the external magnetic field of 6 T. A majority of studies focused on the CMR materials with the doped valence less than +3, i.e. the hole doped manganese oxides.

Received date: May 15, 2017

Foundation item: National Natural Science Foundation of China (61471301, 51402240, 51572222, 51471134)

Corresponding author: Chen Changle, Ph. D., Professor, Shaanxi Key Laboratory for Condensed Matter Structure and Properties, Northwestern Polytechnical University, Xi'an 710129, P. R. China, Tel: 0086-29-88431670, E-mail: chencl@nwpu.edu.cn

Copyright © 2018, Northwest Institute for Nonferrous Metal Research. Published by Elsevier BV. All rights reserved.

Subsequently, S. Das and P. Manda found that Ce doped manganese oxides exhibit CMR effect<sup>[14]</sup>. More importantly, they demonstrated that the CMR effect of these materials originates from the doping  $Ce^{4+}$ , which induces the electron doped CMR effect<sup>[13]</sup>. Mitra<sup>[15]</sup> prepared  $La_{1-x}Ce_xMnO_3$  epitaxial films on  $LaAlO_3$  substrate by PLD technology, and found that the films are single crystal. Compared with the bulk materials, the film exhibits a sharper metal insulator transition peak, larger magnetoresistance, and higher transition temperature with great prospects for practical application of potential.

Although studies on electronic doped thin films have been widely carried in recent years, few investigations in these literatures were focused on transport properties and mechanisms, especially when the external fields were directly applied. This restricted the applications of the electronic doped thin films as the new multi-functional devices. The idea used in our work is to establish the instinct relations between external fields and the electric transport mechanisms in the electronic doped thin films. The switching effect under the magnetic field is expected to be applied to the new energy transducer devices. Moreover, the photoinduced transport properties of electronic doped thin films are investigated, which are reported rarely. That is the novelty in this work. Otherwise, because of the high peak resistivity, the large remanent resistance at low temperatures studies, and the electric localization due to the existence of impurity or disorder phases, preparation of  $La_{1-x}Ce_xMnO_3$  materials is generally difficult. It still needs a lot of work to questioning the feasibility of reliable electron doping for the manganite compounds to investigate this fundamental issue. That is the reason that we choose  $La_{1-x}Ce_xMnO_3$  as the target.

## 1 Experiment

$La_{1-x}Ce_xMnO_3$  ( $x=0.10, 0.20, 0.33$ ) polycrystalline targets were prepared by conventional solid-state reaction process. In the experiments, the raw materials included  $La_2O_3$ ,  $CeO_2$  and  $MnO_2$  (purity not less than 99.99%) with analytical purity. Powders were baked in a muffle furnace for 2 h in order to get dehydrated. According to the required size of the target, the raw materials were chosen for 0.15 mol. The weighted raw materials were ground for 7~8 h, heated up to 1200 °C, thermal insulated for 20 h, and then cooled down. Then the above processes were repeated except for heating up to 1300 °C for 15 h. After several processes of heating, powders were pressed into a wafer with diameter of 40 mm under pressure of 60~70 MPa. The wafer was sintered at 1350 °C for 20 h to finish the preparation of polycrystalline bulk circular target.

Thin film of  $La_{1-x}Ce_xMnO_3$  was grown on a (001) oriented 5 mm×5 mm×0.2 mm STO substrate by pulsed laser deposition technology. Pulsed KrF excimer laser was used with the wavelength of 248 nm and frequency of 2 Hz. During the deposition, the substrate temperature and the oxygen pressure were kept at 800 °C and 10 Pa, respectively. Annealing was carried out in situ at the deposition temperature in oxygen pressure of 30 Pa. Then, the film was cooled down to room temperature slowly at a rate of 5 °C/min. Experimental conditions are specifically listed in Table 1. The thickness was estimated by a SPECEI-2000-VIS ellipsometer. Au poles were put onto the surfaces of  $La_{1-x}Ce_xMnO_3$  film and the substrate acted as electrodes. The structure of film was analyzed by X-ray diffractometer (XRD) using Ni filtered Cu K $\alpha$  radiation operated (RigakuD/max-2400, the wavelength is 0.15432 nm).

Fig.1 shows the XRD patterns of  $La_{1-x}Ce_xMnO_3$ (LCeMO) thin films grown on  $SrTiO_3$ (STO) substrates, with the doping ratio  $x=0.10, 0.20$  and  $0.33$ . It can be seen that the films exhibit perovskite structures in agreement with the orientation of the

Table 1 Preparation parameters of  $La_{1-x}Ce_xMnO_3$ /STO film by PLD

t/min	T/°C	Oxygen pressure/Pa	f/Hz	Energy/mJ	Annealing time, t/min	Annealing oxygen pressure/Pa
60	800	10	2	140	60	30

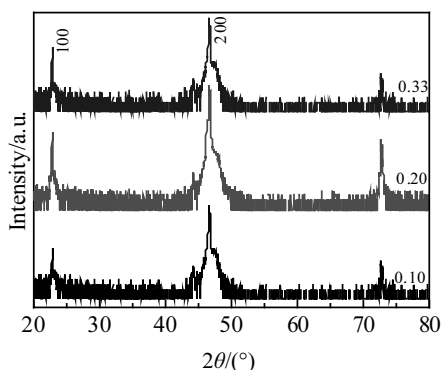


Fig.1 XRD patterns of  $La_xCe_{1-x}MnO_3$ (LCeMO)/ $SrTiO_3$ (STO)

STO and no trace of other impurities and phases can be found, indicating the fine epitaxy of the films. The surface morphologies of LCeMO thin films are shown in Fig.2. It shows the dense and smooth surfaces of all the films. As the doping ratio increases, it appears that the LCeMO film exhibits the smaller grain size and the smoother surface, with the root-mean-square (RMS) roughness of ~5.132, 4.165 and 2.948 nm for  $x=0.10, 0.20, 0.33$ , respectively. This is attributed to the doping of Ce, which is able to enhance the energy of chemical bonds during the crystal growth. As a result, the increase of the doped Ce leads to the more significance of the surface diffusion, which will be responsible for the trend of layer-by-layer growth mode, as well as the promotion of grain refinement.

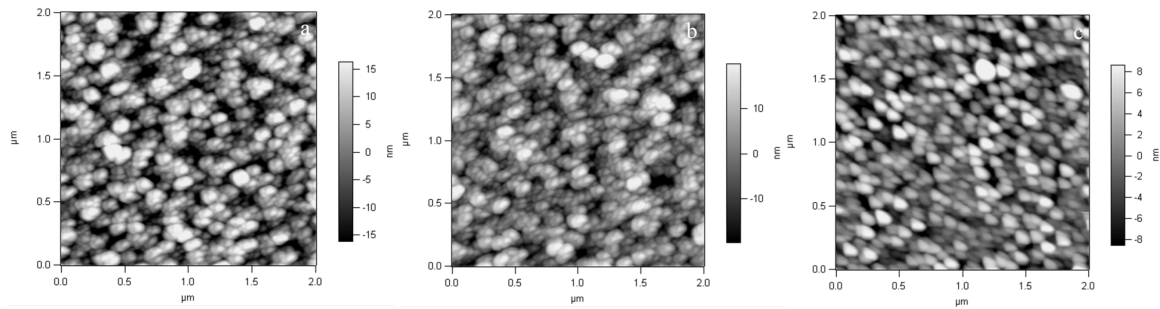


Fig.2 Surface morphologies of  $\text{La}_{1-x}\text{Ce}_x\text{MnO}_3$  thin films: (a)  $x=0.10$ , (b)  $x=0.20$ , and (c)  $x=0.33$

## 2 Results and Discussion

To study the transport properties of the LCeMO films, we firstly investigated the resistance-temperature ( $R$ - $T$ ) curves for the different doping ratios, as shown in Fig.3. It clearly reveals that the films exhibit the well conductive features during the entire region of 50~300 K. In particular, the resistances of all the films undergo the MIT by changing the temperature. The resistances get larger with the increase of temperature in the low temperature region, corresponding to the metal state, while it exponentially decreases with the increase of temperature in the high temperature region, corresponding to the insulator state. The transition temperature rises by increasing the doping ratio of Ce, with the value of 230, 250 and 270 K for  $x=0.10, 0.20, 0.33$ , respectively. This is in good agreement with the Curie temperature  $T_p$  estimated by the previous  $M$ - $T$  measurement, implying that the substitution of La by Ce in  $\text{LaMnO}_3$  induces the MIT accompanied by the occurrence of ferromagnetic ordering and the CMR effect, which can be modulated by the doping ratio.

Further investigations of the transport mechanisms were carried out on the fitting analysis of the  $R$ - $T$  curves in Fig.3. In general, the electric transport properties of thin films at low temperatures can be regarded as the macroscopic reflection of the features of low-energy excited states and the electrons scattering. In the perovskite manganites system, it turns to be more complicated due to the CMR effect, which makes the

electric transport mechanism have different degrees of correlations with the grain boundaries, crystal defects, and magnetic ordering domains. In this paper, we used a typical model of  $R=R_0+R_1T^2+R_2T^{4.5}$  to describe the transport mechanisms of LCeMO at low temperatures, where  $R_0$  represents the resistance induced by the temperature-independent scatterings such as the scattering of magnetic domains<sup>[16,17]</sup>, the item of  $R_1T^2$  represents the scattering of electron-electron, and the item of  $R_2T^{4.5}$  represents the scattering of electron-phonon. It can be seen that the fitting curves are well matched with the experimental measurements, with the fitting parameters shown in Table 2. The fitting results indicate that the magnetic domains and electron-electron scattering mainly contribute to the transport mechanism in the low temperature region. At high temperatures, however, the transport mechanisms can be attributed to the hopping conduction of small polaron, originating from the combined actions of the localized  $e_g$  carriers and lattice distortion. The fitting expression is  $R=A\text{Texp}(E_a/k_B T)$ , where  $E_a$  is the activation energy of the small polaron hopping. It can be seen that  $E_a$  increases with the increase of  $x$ , suggesting that the raised ratio of the doped Ce has reduced the average A-site cation radius, enhanced the Jahn-Teller dislocation, and leads to further localization of carriers. This will impose the restrictions on the thermodynamic hopping of the small polarons, consequently yielding the larger values of the activation energy.

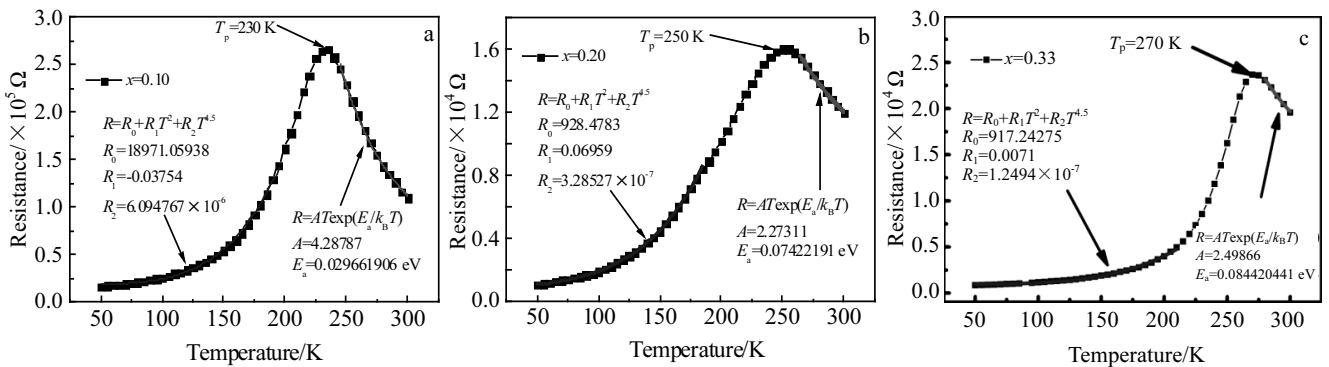


Fig.3 Resistance-temperature ( $R$ - $T$ ) curves and fitting analysis for the different doping ratios in  $\text{La}_{1-x}\text{Ce}_x\text{MnO}_3$  thin films: (a)  $x=0.10$ , (b)  $x=0.20$ , and (c)  $x=0.33$

**Table 2 Fitting parameters of  $R$ - $T$  curves of  $\text{La}_{1-x}\text{Ce}_x\text{MnO}_3$  films in the low temperature region**

Substrate	$\text{La}_{1-x}\text{Ce}_x\text{MnO}_3$	$R_0$	$R_1$	$R_2/\times 10^{-7}$
STO	$x=0.10$	18971.06938	-0.03754	60.94767
	$x=0.20$	928.4783	0.06959	3.28527
	$x=0.33$	917.24275	0.0071	1.2494

The photo induced transport properties can be observed under the light illumination. Measurements began after 20 s of radiation in order to avoid the relaxation dynamic processes. Fig.4 displays the photo-resistances as a function of the temperature with the light intensity of 40, 60, 80, 100 and 120 mW for  $x=0.10, 0.20$  and  $0.33$ . We defined the relative change in the photo-induced resistance by  $\Delta R/R=(R_L-R)/R\times 100\%$ , where  $R_L$  represents the photo-resistance under the light illumination, and  $R$  is the dark resistance without irradiation. It shows that the  $\text{La}_{1-x}\text{Ce}_x\text{MnO}_3$  film exhibits MIT at  $T_m=230, 250,$  and  $270$  K for  $x=0.10, 0.20$  and  $0.33$ , respectively. Below  $T_m$ , light-induced relative change in the resistance increases by increasing temperature, while it decreases with the temperature above  $T_m$ . At the same temperature, the higher laser intensity gives rise to the more significant change in resistance.

It can be noted that laser irradiation was found to induce the shift of metal insulator transition temperature  $T_m$  towards the

lower temperature region. Resistances of samples increase with the higher laser intensity in the low temperature region, while they decrease by enhancing the laser during the region above the transition temperature. This can be interpreted by the coexistence of ferromagnetic (FM) metallic phase and paramagnetic (PM) insulating phase in LCeMO films. The transport of doped manganite is closely related to the spin system of  $e_g$  carriers and localized  $t_{2g}$  spin core in Mn ions. In the PM state, the transport mechanism of LCeMO is attributed to hopping conduction of the small polaron, originating from the combined actions of the localized  $e_g$  carriers and lattice distortion. Light can excite more photo induced carriers, and enhance the hopping of small polarons, leading to the increase of photoconductivity. In the metallic phase, however, the photo induced demagnetization effect will play a dominant role. Light can excite spin-down  $e_g$  electrons, which are expected to destroy the FM coupling between spin-up  $e_g$  and  $t_{2g}$  electrons in Mn ions. As a result, the DE effect of LCeMO is weakened, leading to the increase of the photo induced resistance.

The  $R$ - $T$  curves of  $\text{La}_{1-x}\text{Ce}_x\text{MnO}_3/\text{STO}$  thin film samples were measured under the external magnetic field (0~0.8 T), as shown in Fig.5. The inset of Fig.5 illustrates the corresponding relation between the magnetoresistance and temperature ( $MR$ - $T$ ). It can be observed that the doping  $x=0.10$

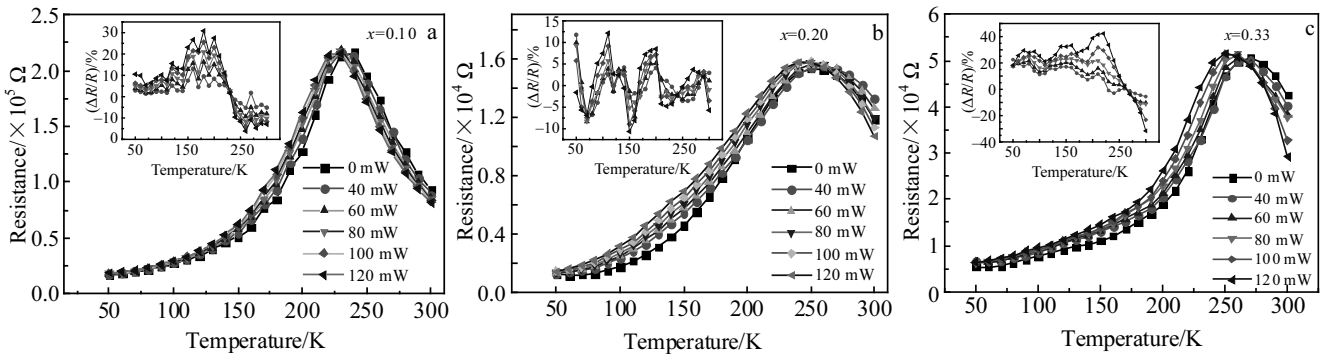


Fig.4 Photo induced resistances as a function of temperature with the light intensity of 0, 40, 60, 80, 100 and 120 mW for the different doping ratios in  $\text{La}_{1-x}\text{Ce}_x\text{MnO}_3$  thin films: (a)  $x=0.10$ , (b)  $x=0.20$ , and (c)  $x=0.33$

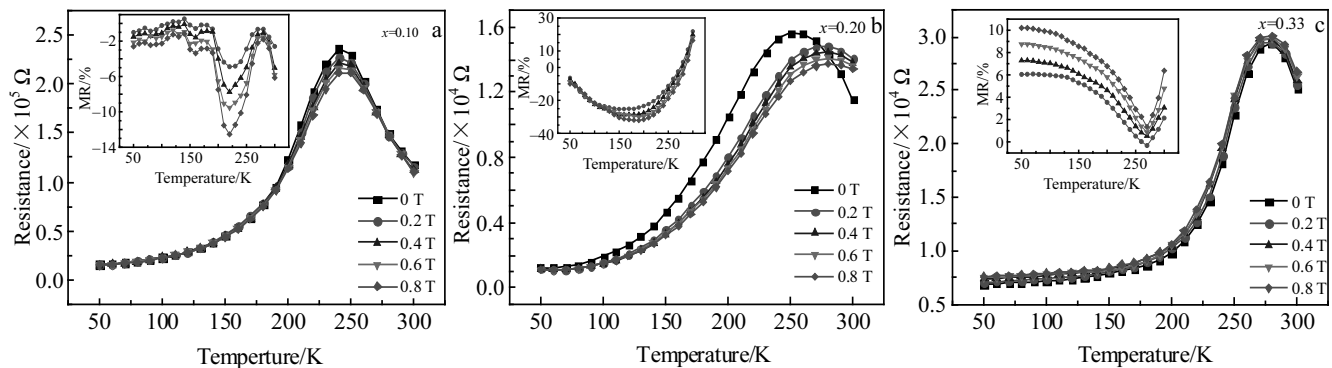


Fig.5  $R$ - $T$  curves and magnetic-resistance ( $MR$ ) versus temperature curves (inset) under the external magnetic field of 0, 0.2, 0.4, 0.6, 0.8 T for the different doping ratios in  $\text{La}_{1-x}\text{Ce}_x\text{MnO}_3$  thin films: (a)  $x=0.10$ , (b)  $x=0.20$ , and (c)  $x=0.33$

sample exhibits negative magnetoresistance effect in the entire temperature region. In particular, MR increases with the increase of temperature for  $T < 230$  K, and it reaches the peak value of  $MR = 13.5\%$  at  $T_m = 230$  K. In the temperature range of  $T > 230$  K, MR gradually declines with the temperature. For the doping concentration of  $x = 0.20$ , the magnetoresistance effect undergoes a significant crossover from positive to negative when the temperature is up to a critical value. At lower temperature, the sample shows the enhanced negative MR effect with the higher temperature and reaches to the peak value of  $MR = 30.5\%$  at  $T = 200$  K. For the higher temperature ( $T > 200$  K), the MR effect is weakened with the increase of temperature until the switching effect occurs at 250 K. After that, the sample shows the continually increased positive MR effect by increasing the temperature. When  $x = 0.33$ , however, the resistance of the thin film sample exhibits the lower values under the higher magnetic field, corresponding to the positive magnetoresistance effect. The value of MR increases by raising the magnetic field. With the increase of the temperature, the performance of MR firstly decreases and then increases. The valley value of magnetoresistance falls down to  $MR = 0\%$  at  $T = 270$  K and magnetic field of 0.2 T. Peaks and valleys in MR- $T$  curves are related to the MIT transition for different doping cases. The switching effect actually reflects different coupling mechanisms between spins and orbits in LCeMO films.

### 3 Conclusions

1) In the  $R$ - $T$  curves,  $La_{1-x}Ce_xMnO_3$  films exhibit the significant metal-insulator transition, the transition temperature rises with increasing the doping ratio of Ce.

2) The magnetic domains and electron-electron scattering mainly contribute to the transport mechanism in the low temperature region, while the hopping conduction of small polaron becomes the dominating factor at the high temperatures.

3) Laser irradiation induces the shift of metal insulator transition temperature  $T_m$  towards the lower temperature

region. Moreover, the higher laser intensity gives rise to the more significant changes in resistance.

4) The doping ratio modulated MR effect can be attributed to the MIT transition and different coupling mechanisms between spins and orbits in LCeMO films.

### References

- 1 Niu L W, Chen C L, Dong X L et al. *Chinese Physics B*[J], 2016, 25 : 107 701
- 2 Lo S T, Lin S W, Wang Y T et al. *Scientific Reports*[J], 2014, 4: 5438
- 3 Wang Q Y, Lin H Y, Wang S R et al. *Applied Physics Letters*[J], 2016, 108(20): 202 403
- 4 Qiang G, Fang Y, Lu X et al. *Applied Physics Letters*[J], 2016, 108(2): 22 906
- 5 Nan C W, Bichurin M, Dong S et al. *Journal of Applied Physics*[J], 2008, 103: 31 101
- 6 Lu C, Hu W, Tian Y et al. *Applied Physics Reviews*[J], 2015, 2(2): 21 304
- 7 Shaykhtudinov K A, Nikitin S E, Petrov M I et al. *Journal of Applied Physics*[J], 2015, 117(16): 163 918
- 8 David A, Tian Y F, Yang P et al. *Scientific Reports*[J], 2015, 5: 10 255
- 9 Zhang J Y, Kim H, Mikheev E et al. *Scientific Reports*[J], 2016, 6: 23 652
- 10 Li W, Dong X, Wang S et al. *Applied Physics Letters*[J], 2016, 109: 91 907
- 11 Chai X J, Xing H, Jin K X. *Scientific Reports*[J], 2016, 6: 23 280
- 12 Von Helmolt R, Wecker J, Holzapfel B et al. *Physical Review Letters*[J], 1993, 71: 2331
- 13 Jin S, Tiefel T H, McCormack M et al. *Science*[J], 1994, 264: 413
- 14 Mandal P, Das S. *Physics Review B*[J], 1997, 561(23) : 15 073
- 15 Mitra C, Raychaudhuri P, John J et al. *Journal of Applied Physics*[J], 2001, 89(1): 524
- 16 Agarwal V, Sharma G, Siwach P et al. *Applied Physics A*[J], 2015, 119: 89
- 17 Khan M H, Pal S. *Applied Physics A*[J], 2015, 119: 1443

## 不同 Ce 掺杂比的 $La_{1-x}Ce_xMnO_3$ 薄膜输运性质及机理研究

牛利伟, 陈长乐, 王建元, 金克新

(西北工业大学 陕西省凝聚态结构与性质重点实验室, 陕西 西安 710129)

**摘要:** 研究了电子型掺杂钙钛矿薄膜  $La_{1-x}Ce_xMnO_3$  的输运性质和外场作用下的输运机理。研究表明,  $La_{1-x}Ce_xMnO_3$  薄膜呈现出典型的金属-绝缘体转变, 且与 Ce 的掺杂浓度相关。电阻-温度曲线表明, 在低温时, 电子-电子散射和磁畴对电子的散射是电阻形成的主要原因, 而在高温下, 小极化子的跳跃机制起主要作用。通过激光照射样品表面, 发现光场诱导金属-绝缘体转变温度向着低温区偏移, 该现象产生的原因在于  $La_{1-x}Ce_xMnO_3$  薄膜内部铁磁相与顺磁相的共存, 此外, 高能量的激光对样品的电阻变化影响更明显。进一步研究表明, Ce 的掺杂浓度将会通过金属-绝缘相变对  $La_{1-x}Ce_xMnO_3$  薄膜的磁电阻效应产生显著的调制作用。

**关键词:** 钙钛矿锰氧化物; 输运机理; 金属-绝缘体转变; 巨磁电阻效应

作者简介: 牛利伟, 男, 1984 年生, 博士生, 西北工业大学应用物理系, 陕西 西安 710129, 电话: 029-88431670, E-mail: 2009100479@mail.nwpu.edu.cn